ISSN 1028-334X, Doklady Earth Sciences, 2006, Vol. 406, No. 1, pp. 141–147. © Pleiades Publishing, Inc., 2006.
Original Russian Text © A.A. Marakushev, S.A. Marakushev, 2006, published in Doklady Akademii Nauk, 2006, Vol. 406, No. 4, pp. 521–527.

GEOCHEMISTRY

PT Facies of Elementary, Hydrocarbon, and Organic Substances in the C–H–O System

Academician of the RAS A. A. Marakushev[1] and S. A. Marakushev[2]

Received September 8, 2005

DOI: 10.1134/S1028334X0601034X

The substances in the C–H–O system are subdivided into elementary (O_2, H_2, H_2O, C, CO, CO_2, CH_4) and composite (hydrocarbons and organic compounds) varieties (Fig. 1). The composite substances fit into the system of elementary substances and are located on tie lines that connect their compositions. Owing to this, the three-component system C–H–O is divided into two-component subsystems where hydrocarbons and organic compounds are formed from elementary substances autonomously. The compositions of some organic substances are located at the tie line intersections, which determine their belonging to two (HCOOH) or even three (CH_2O) subsystems. Formaldehyde CH_2O and some of its stoichiometric polymers, listed in Fig. 1, occupy a central position among organic compounds.

The reactions between elementary substances and the free energies ΔG_T^0 of these reactions, calculated from reference book [1], are presented in Table 1. They are equilibrated at each given temperature by the sum of relative chemical potentials ($\mu^p = RT\ln P$) of the substances that participate in these reactions. Assuming the ideal state of gases, these potentials may be summed up with determination of the excess chemical potential that balances the free energy of reactions. For example, in the reaction $CO + 3H_2 = CH_4 + H_2O$, $\Delta G_T^0 = \mu_{CO} + 3\mu_{H_2} - \mu_{CH_4} - \mu_{H_2O} = 2\mu^p = 2RT\ln P$. As a result, the logarithm of the respective equilibrium pressure $\ln P$ is determined as $\Delta G_T^0/2RT$. The reactions presented in Table 1 were used to calculate facies of elementary substances (Fig. 2) for their gas standard state as accepted in thermodynamics and for free carbon as graphite that occurs in the dispersed state in gas mixtures. The volume of carbon atoms is incommensurably small in comparison with gas molecules.

The parageneses of elementary substances shown in Fig. 2 as triangles for each facies are divided into two families that are coordinated by invariant points at 1097 and 1340 K. According to the prevalent paragenesis of elementary substances, they may be termed the water–carbon dioxide and water–methane families, respectively. These families appeared in the geological history as a result of a diverse disproportionation of components of hydrogen-bearing fluids (H_2 + CO) released from the melted Earth's core [2] in various geodynamic settings.

The generation of water–carbon dioxide fluids was facilitated by the extension of the Earth's crust, which decreases the fluid pressure owing to the selective migration of hydrogen as the most mobile component into the atmosphere. As a result, the oxygen-bearing components became prevalent over hydrogen, so that the disproportionation of components led to the generation of water–carbon dioxide fluids according to the reaction $H_2 + CO = H_2O + 0.5CO_2 + 1.5C$, which corresponds to an invariant point at 1097 K (Fig. 2). The water–carbon dioxide fluids are aggressive in relation to sialic (granitic) crustal material, which is leached under their influence, giving rise to the formation of platform or shelf depressions filled with sedimentary or volcanosedimentary rocks. The fluid melting of mantle material contemporaneously proceeded at a depth. The primary melts arising thereby underwent mafic–ultramafic separation with eruptions of fractionated tholeiitic basalts. Ultramafic magmas were emplaced into the base of the crust, with an uplift of the underlying mantle (Moho discontinuity) that is a typical process in depressions. The combination of these processes resulted in the formation of the inversed topography of the depressions underlain by the thinned crystalline crust.

The cessation of tholeiitic basaltic eruptions in the depressions was systematically followed by the deposition of carbonaceous sediments therein. The subsequent explosive alkaline volcanism was accompanied by an uplifting and reverse faulting of the crystalline basement in the depressions. These processes indicate a

[1] *Institute of Experimental Mineralogy, Russian Academy of Sciences, Chernogolovka, Moscow oblast, 142432 Russia*
[2] *Institute of Problem of Chemical Physics, Russian Academy of Sciences, Chernogolovka, Moscow oblast, 142432 Russia; e-mail: marak@cat.icp.ac.ru*

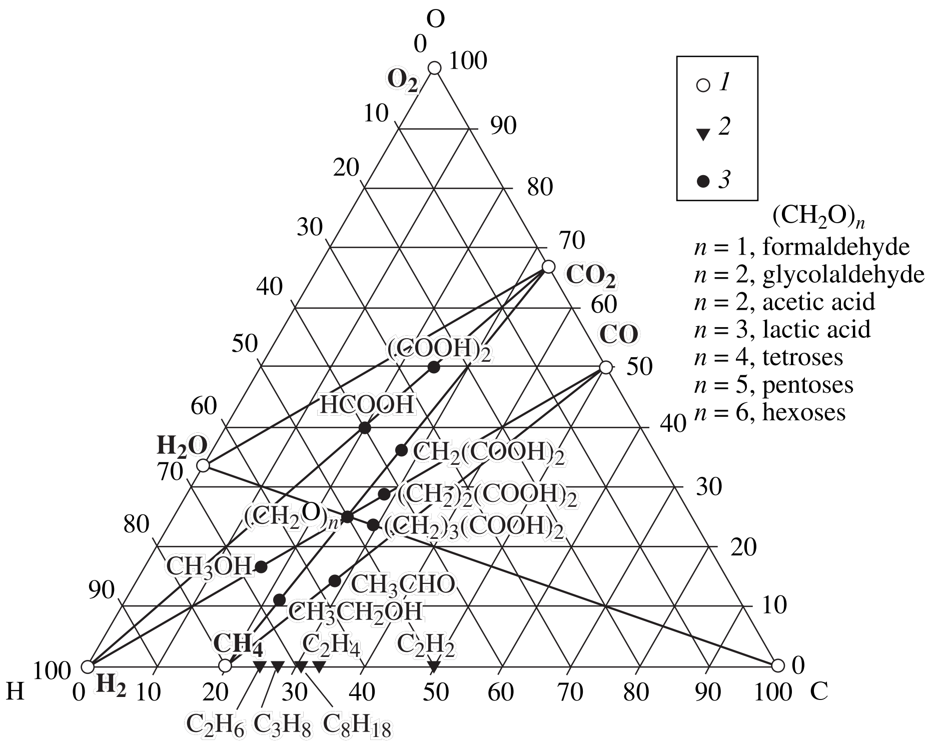

Fig. 1. Compositions of substances in the C–O–H system. (*1*) Elementary substances; (*2*) hydrocarbons: ethane C_3H_6, propane C_3H_8, octane C_8H_{18}, ethylene C_2H_4, and acetylene C_2H_2; (*3*) organic compounds: methanol CH_3OH, formaldehyde CH_2O, formic acid HCOOH, ethanol CH_3CH_2OH, acetaldehyde CH_3CHO, oxalic acid $(COOH)_2$, malonic acid $CH_2(COOH)_2$, siccine acid $(CH_2)_2(COOH)_2$, and glutaric acid $(CH_2)_3(COOH)_2$. The listed CH_2O polymorphs are located at intersections of three tie lines that connect elementary substances.

compressive environment of the Earth's crust, preventing the migration of hydrogen from ascending fluid flows. The consequent recovery of the initial state of the prevalence of hydrogen over oxygen-bearing components drastically changed the reaction of disproportionation of components $4H_2 + 2CO = 2H_2O + CH_4 + C$. The reaction included elementary substances that correspond to an invariant point at 1340 K (Fig. 2). As a result, the evolution of the fluid regime of volcanic activity is displayed by the facies combined by invariant points 1097 → 1340 K (Fig. 2).

This evolution is reflected in the intrusive magmatism of depressions localized in the sedimentary sequences that separate the lower and upper tholeiitic basalts. The alkaline intrusions that complete geological cycles in the development of depressions differ from other igneous rocks, which commonly contain inclusions of water–carbon dioxide fluids, by the abun-

Table 1. ΔH^0_{298} and ΔG^0_T values, kJ/mol of reactions between elementary substances in gas phase

Reaction	ΔH^0_{298}	ΔG^0_T				
		298 K	600 K	900 K	1200 K	1500 K
$C + 2H_2 = CH_4$	−74.81	−50.71	−22.80	8.72	41.64	75.05
$CO + 3H_2 = CH_4 + H_2O$	−206.09	−142.16	−72.3	2.06	78.04	154.40
$CH_4 + 2CO = 3C + 2H_2O$	−187.80	−132.09	−76.22	−22.04	31.16	83.66
$CO_2 + 2H_2 = C + 2H_2O$	−90.12	−62.76	−32.81	−0.39	33.28	67.56
$2CO = CO_2 + C$	−172.45	−120.03	−66.20	−12.92	39.51	91.12
$CO + H_2 = C + H_2O$	−131.28	−90.86	−49.51	−6.66	36.40	79.35
$CO + H_2O = CO_2 + H_2$	−41.17	−28.63	−16.69	−6.27	3.11	11.77
$CH_4 + CO_2 = 2C + 2H_2O$	−15.31	−12.06	−10.01	−9.11	−8.35	−7.46

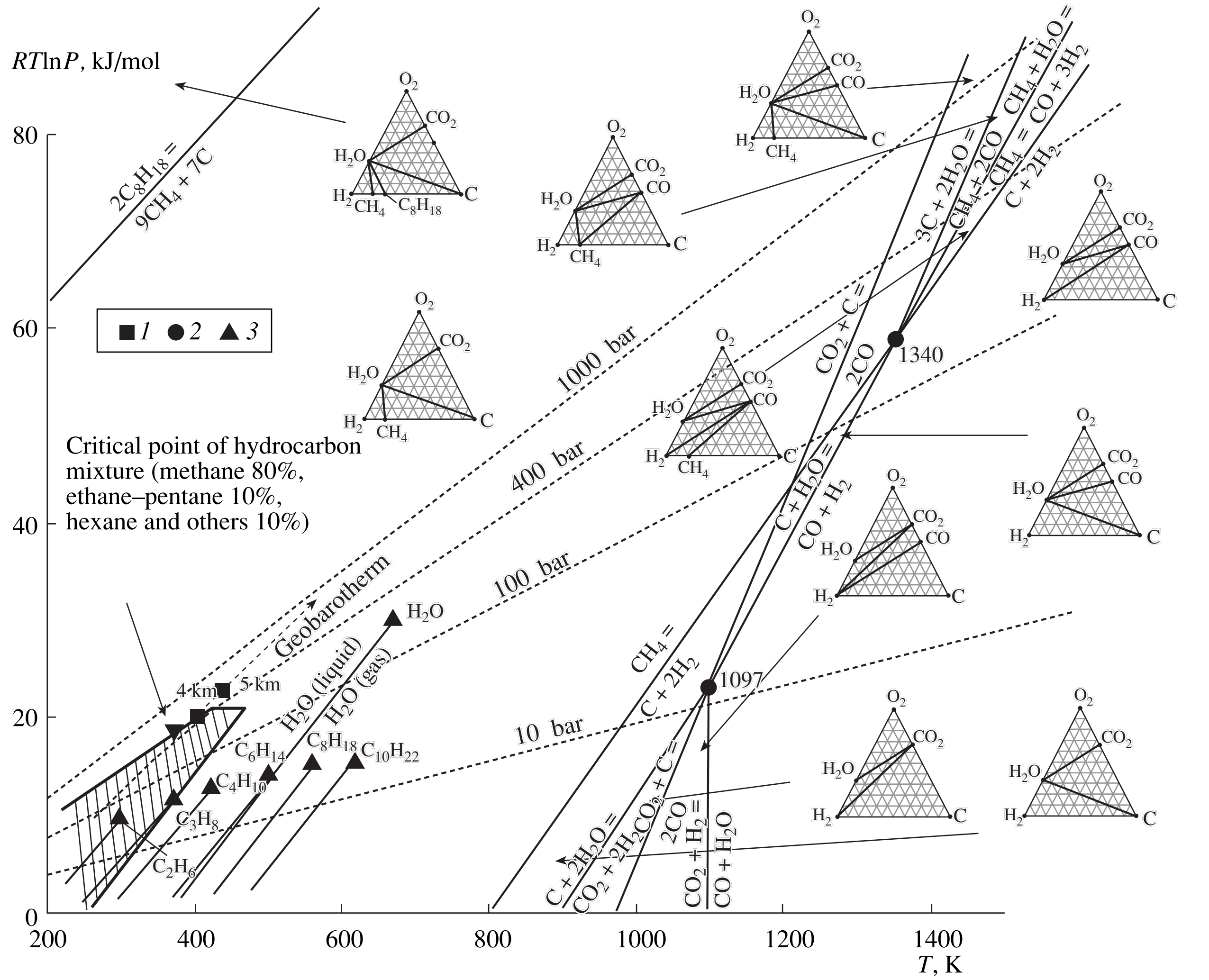

Fig. 2. Facies of elementary substances in the C–H–O system and *n*-octane C_8H_{18}. The region of common occurrence of gas and oil pools in the Earth's crust [11] is hatched. (*1*) Depths in the Earth's crust along geobarotherm; (*2*) invariant equilibria; (*3*) critical points of hydrocarbons [4] and water. Isobars are shown by dashed lines.

dant fluid inclusions filled with methane and heavier hydrocarbons. Methane fills amygdules in alkaline volcanic rocks and basalts, including those dated back to 3.8 Ga [3]. Isobars of 100–1000 bar, shown in Fig. 2, depict a vast region of variations in the paragenesis of fluid flows, from the initial high-temperature facies to the low-temperature ($CH_4 + H_2O$) facies related to the invariant equilibrium at 1340 K.

The ($CH_4 + H_2O$) paragenesis is also inherent to the gas and oil pools that are formed in the Earth's crust at *PT* parameters below the critical point, largely in the hatched region in Fig. 2. As in all other accumulations of methane in the crust, these pools contain heavy hydrocarbons, the genetic relations of which with methane represent an important problem. The stability field of octane n-C_8H_{18} shown in Fig. 2 constrains the (methane + carbon) association at a high pressure, far above its critical pressure. The relationships of methane with ethane, propane, and ethylene are demonstrated by the diagram of the two-component C–H system (Fig. 3). The reactions that correspond to monovariant equilibria in this system are presented in Table 2 together with other reactions calculated for Fig. 4 considered below. The free energies ΔG_T^0 of the reactions and their enthalpies ΔH_{298}^0 were determined from the data reported in [4, 5].

The diagram shown in Fig. 3 demonstrates the deep origin of heavy hydrocarbons, the facies of which are juxtaposed to a great extent with the stability field of diamond that replaces graphite at a depth of ~150 km (based on geobarotherm). The deep origin of heavy HCs is supported also by their occurrence in methane inclusions captured by diamond [6] and ultramafic rocks genetically related to the mantle sources [7]. The relationship of heavy HCs with deep mantle magma-

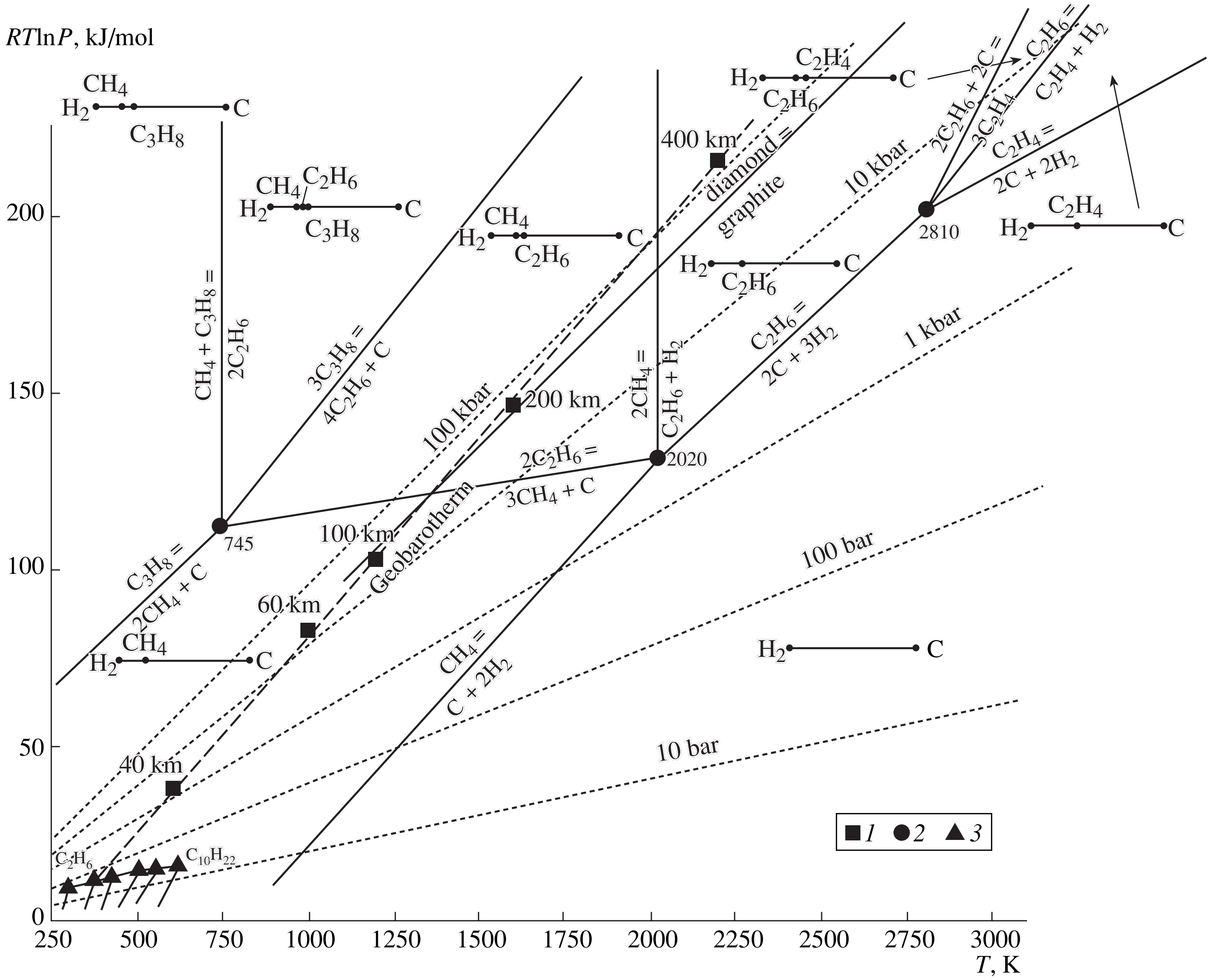

Fig. 3. Hydrocarbon facies in the two-component C–H system. (*1*) Depths in the Earth's crust along geobarotherm [9]; (*2*) invariant equilibria; (*3*) critical points of hydrocarbons C_2H_6–$C_{10}H_{22}$ [4]. Isobars are shown by dashed lines. (CH_4) Methane, (C_2H_6) ethane, (C_2H_4) ethylene, (C_3H_8) propane.

tism was discussed in [5, 8, 9]. "The increase in the stability of heavy HCs with pressure and their breakdown resulting in the formation of CH_4 with pressure drop, when magmas intrude the Earth's crust" was emphasized in [10, p. 252].

The facies relationship (Fig. 3) shows that the heavy HCs are stable only under a high pressure and that they are displaced by methane with a decrease in pressure. However, they occur in gas and oil pools that are formed in the upper crust below the critical parameters (Fig. 2). These relationships indicate a supply of metastable heavy HCs with fluids from their deep sources. By the thermodynamic properties, hydrocarbons make up systematic successions [Helgeson *et al.*, 1998]. The most abundant saturated hydrocarbons are disposed as the following series (in order of increasing free energy ΔG^0_{298} and decreasing enthalpy ΔH^0_{298} of formation, kJ/mol): methane CH_4 (–50.71; –74.81), ethane C_2H_6 (–32.96; –84.52), propane C_3H_8 (–24.63; –105.15), *n*-butane (–16.26; –125.78), *n*-pentane C_5H_{12} (–7.81; –146.48), *n*-hexane C_6H_{14} (+0.47; –167.04), *n*-heptane C_7H_{16} (+6.84; –187.67), *n*-octane C_8H_{18} (+17.2; –208.30). This series reflects the succession of reactions of their formation from elements ($C + 2H_2 = CH_4 \to 8C + 9H_2 = C_8H_{18}$) with decreasing temperature and increasing pressure. Unsaturated hydrocarbons have the positive parameters mentioned above [5], for example, ethylene C_2H_4 (68.07; 52.23) and acetylene C_2H_2 (208.97; 226.51). The extremely high formation temperatures are calculated from these parameters (see Fig. 3 for C_2H_4). Facies of hydrocarbons (Fig. 3) are characterized by the following combinations: methane and carbon, methane and ethane, methane and propane, ethane and propane, hydrogen and ethane, ethane and ethylene, hydrogen and ethylene. Parageneses of these HCs together with other heavy HCs originated from elementary sub-

Table 2. ΔH^0_{298} and ΔG^0_T values, kJ/mol of reactions of elementary substances with hydrocarbons (ethane C_2H_6, propane C_3H_8, *n*-octane C_8H_{18}, and ethylene C_2H_4) and organic compound (acetic acid CH_3COOH) in gas phase

Reaction	ΔH^0_{298}	ΔG^0_T				
		298 K	900 K	1200 K	1500 K	1800 K
$2C + 3H_2 = C_2H_6$	–84.52	–32.96	71.20	123.10	175.01	226.92
$3CH_4 + C = 2C_2H_6$	55.39	86.21	116.24	121.28	124.87	128.13
$2CH_4 + C = C_3H_8$	44.47	76.79	120.59	135.81	150.05	164.07
$4C_2H_6 + C = 3C_3H_8$	22.63	57.95	129.29	164.87	200.41	235.95
$2C_2H_6 = CH_4 + C_3H_8$	–10.92	–20.34	4.35	14.53	25.18	37.14
$C_2H_6 + H_2 = 2CH_4$	–65.10	–68.46	–53.76	–39.82	–24.91	–9.08
$10C_2H_6 + CO_2 = 7C_3H_8 + 2H_2O$	19.03	94.43	253.82	335.91	418.54	501.49
$5C + 4H_2O = C_3H_8 + 2CO_2$	75.09	100.90	138.81	152.53	164.97	176.78
$7C + 6H_2O = 2C_2H_6 + 3CO_2$	101.47	122.59	144.51	147.67	148.97	151.29
$C_2H_6 + 3CO = 5C + 3H_2O$	–309.33	–241.34	–91.64	–14.57	62.05	138.43
$7CO + 3H_2O = C_2H_6 + 5CO_2$	–552.97	–358.93	54.55	211.46	394.12	571.81
$5CH_4 + CO = 3C_2H_6 + H_2O$	16.21	63.27	163.34	197.5	229.13	263.08
$7C_2H_6 = 6CH_4 + C_8H_{18}$	–65.52	–56.34	26.66	87.89	152.00	216.76
$3C_2H_6 + 2C = C_8H_{18}$	45.26	116.08	259.14	330.45	401.74	473.02
$9CH_4 + 7C = 2C_8H_{18}$	256.69	490.77	867.02	1024.7	1178.1	1330.43
$2C + 2H_2 = C_2H_4$	52.42	69.12	100.07	116.02	131.96	147.91
$C_2H_4 + H_2 = C_2H_6$	–136.94	–102.08	–28.87	7.08	43.14	79.01
$3C_2H_4 = 2C_2H_6 + 2C$	–326.30	–273.28	–157.8	–100.5	–44.18	12.13
$2C + 2H_2O = CH_3COOH$	49.75	81.36	137.67	162.82	187.20	211.12
$C_3H_8 + 2CO_2 = 2CH_3COOH + C$	24.41	61.82	136.54	173.13	209.43	245.47
$2C_2H_6 + CO_2 = CH_3COOH + C_3H_8$	23.52	59.88	133.91	169.00	204.92	240.65
$4CO_2 + 2C_3H_8 + 2H_2O = 5CH_3COOH$	98.57	205.00	410.75	509.09	606.06	702.06
$6CO_2 + 4C_2H_6 + 2H_2O = 7CH_3COOH$	145.61	324.33	671.49	844.45	1012.65	1179.45
$CH_3COOH + 8C_2H_6 = 6C_3H_8 + 2H_2O$	–4.49	34.54	120.91	166.91	213.62	260.78

Note: Reactions correspond to the zero or negative volumetric effect.

stances in the hydrogen fluid flows that ascend in a pulsatory manner from the melted Earth's core.

The fluid flows removed HCs from their deep sources and transported them into the Earth's crust in a metastable state. In the extensive methane–carbon facies, the heavy HCs are retained in the Earth's crust only as relicts far beyond the fields of their thermodynamic stability (facies). Below the critical temperature and pressure, the metastable fluid hydrocarbon mixtures are separated into gas and liquid phases (Fig. 2), eventually leading to the formation of oil pools degassed to a variable extent and to the appearance of overlying gas pools of higher migration ability [11, 12]. The fluid influx of hydrocarbons in the Earth's crust leading to the formation of oil and gas pools was periodically reinforced during short periods of geological history in the Paleoproterozoic, Neoproterozoic, Paleozoic, and Cenozoic [13]. Oil generation continues today and compensates the exhaustion of the older oil pools [12]. According to [14], the accumulation of metastable heavy HCs generates earthquake centers in the crust and the mantle. Oil generation in the geological history reflects the pulsatory degassing of the liquid Earth's core in the course of the discrete endogenic activity of the Earth [2].

The oil and gas fields are localized in depressions of the platform and shelf zone of the continental folded crust. The oil generation is related to the final stage of their development, which is characterized by uplifts and reverse faulting of the crystalline basement. Numerous examples of the structural control of oil fields in shelf depressions of South Vietnam are discussed in [12]. For instance, the Oligocene–Pleistocene Hue shelf basin is underlain by the Devonian limestone. The White Pheasant oil and gas field in this basin is controlled by a reverse fault in the basement. It may be

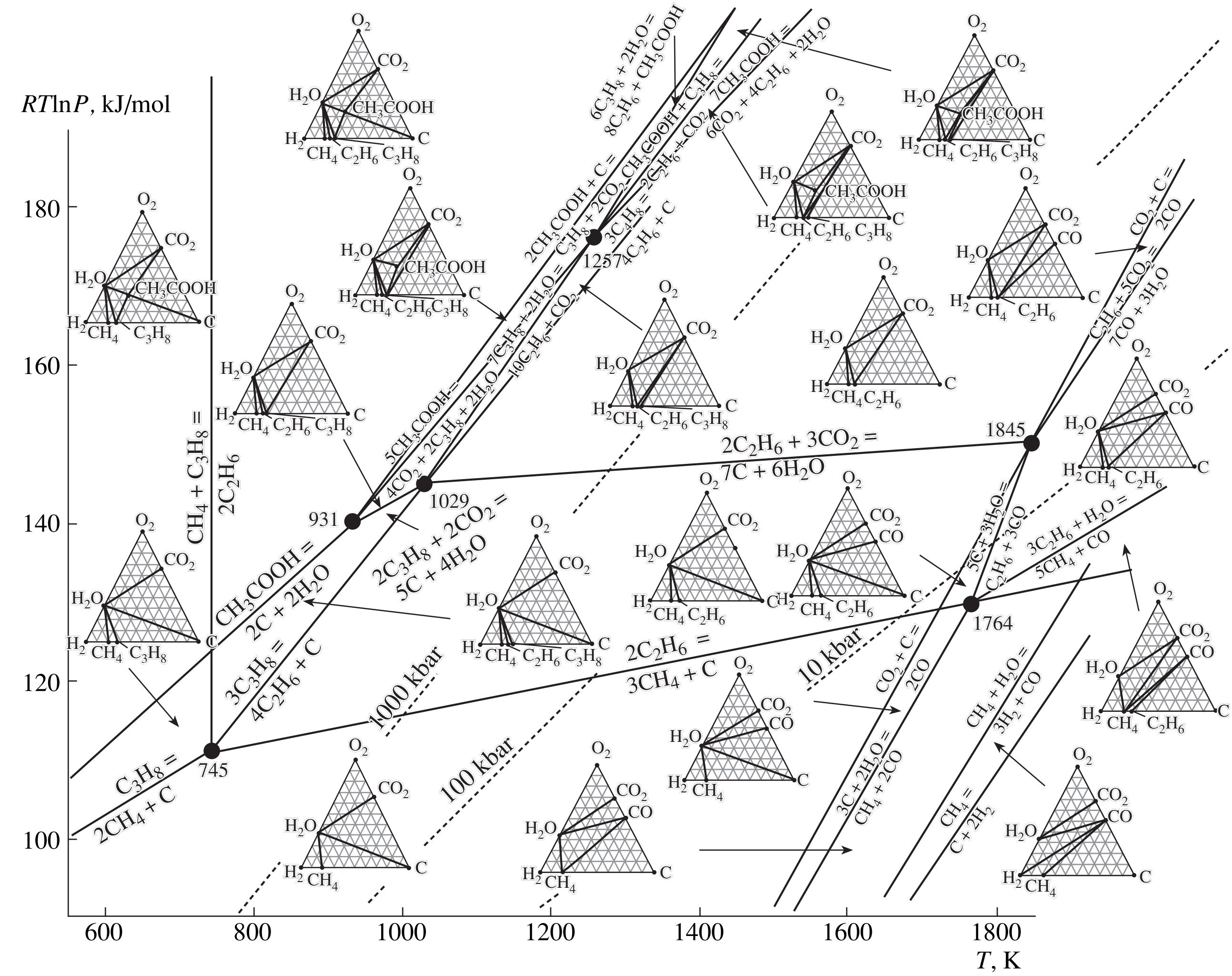

Fig. 4. Facies of elementary substances, hydrocarbons, and organic compound (acetic acid CH_3COOH). See Fig. 2 for legend.

suggested that the initial filtration of the aggressive high-temperature above-critical fluid (Figs. 2, 3) leached the limestone and created chambers that were subsequently filled with oil when the temperature of fluid fell below the critical point. The oil pools were localized in the upthrown limestones, whereas gas migrated upward and accumulated in the overlying Oligocene clay. In the Khuolong Basin (southern Konshon area), the crystalline basement consists of granites. Their deep reverse faulting controlled the oil pools, which are mainly hosted in sedimentary rocks and only partly extend into the upthrown granites. The White Tiger field displays a fundamental distinction. The giant oil pools of this field are mainly hosted in the stepwise reverse fault zone within granites, extending down to a depth of 1.5 km and only partly penetrating into the adjacent and overlying sedimentary beds [12]. In this case, the impact of the above-critical high-temperature CO_2–water fluids on the granites predated the process of oil formation and leached large cavities, which were subsequently filled with oil when the temperature of hydrocarbon fluids fell below the critical level. The explosions that accompanied these processes led to the brecciation of granites and their cementation by condensed oil, promoting the reverse faulting in the basement of depressions.

The generation of heavy HCs in deep zones of the Earth was conjugated with the formation of organic compounds and the juxtaposition of their facies. Figure 4 shows the example of the gaseous acetic acid CH_3COOH ($\Delta H^0_{298} = -433.88$ kJ/mol, $\Delta G^0_{298} = -375.78$ kJ/mol) on the basis of the equilibria that correspond to the reaction presented in Table 2. The formation of heavy HCs (C_2H_6 and C_3H_8 in this case) stabilizes the organic compounds and expands the fields of their stability. In particular, the gaseous acetic acid is formed as a result of the reactions $2C_3H_8 + 4CO_2 + 2H_2O = 5CH_3COOH$ and $4C_2H_6 + 6CO_2 + 2H_2O = 7CH_3COOH$. The direct synthesis of acetic acid from elementary substances according to reaction $2C + 2H_2O = CH_3COOH$ is more difficult. Nevertheless, this reaction indicates the natural position of acetic acid and other organic compounds in the C–H–O system. The compositions of these compounds are located on tie lines that connect the compositions of elementary substances (Fig. 1). The formation of organic compounds brings about an additional ordering in the C–O–H system, diminishes its entropy, and thus, in the evolution of inorganic matter, approaches the definition of life as envisaged by Schödinger's principle of "order from disorder." The juxtaposition of facies of gaseous organic compounds with hydrocarbon facies (Fig. 4) allows us to suggest their similar genesis, which was favored by pulses of degassing of the Earth's core that are recorded in maximums of oil and gas pool formation in the geological history [13]. The removal of organic compounds to the surface should promote the origin of life within a narrow temperature range of liquid water stability (Fig. 2). Such a regime was maintained on the Earth by the so-called carbonate–silicate cycle, which is provided by the interaction between the hydrosphere and the atmosphere. In this respect, the Earth is a unique planet—the sole cradle of life in the solar system, as provided by its optimal position relative to the Sun in the so-called permanently inhabited zone. As was pointed out in [15], attempts to substantiate the existence of life in space are without prospects, despite the wide abundance of abiogenic organic matter therein.

REFERENCES

1. R. A. Robie and B. S. Hemingway, *Thermodynamic Properties of Minerals and Related Substances at 298.15 K and 1 Bar (105 Pascals) Pressure and Higher Temperatures* (US Geological Survey, Denver, 1995).
2. A. A. Marakushev, *Origin of the Earth and Nature of Its Endogenic Activity* (Nauka, Moscow, 1999) [in Russian].
3. J. L. R. Touret, Precambr. Res. **126**, 219 (2003).
4. H. C. Helgeson, C. E. Owens, A. M. Knox, and L. Richard, Geochim. Cosmochim. Acta **52**, 985 (1998).
5. V. S. Zubkov, *Thermodynamic Modeling of the C–H–N–O–S System at PT Conditions of the Upper Mantle* (Irkutsk State Univ., Irkutsk, 2005) [in Russian].
6. E. Yu. Buslaeva and M. I. Novgorodova, *Elementorganic Compounds and Problem of Ore Matter Migration* (Nauka, Moscow, 1983) [in Russian].
7. T. N. Tingle and M. F. Hochella, Geochim. Cosmochim. Acta **57**, 3245 (1993).
8. R. Sugisaki and K. Mimura, Geochim. Cosmochim. Acta **58**, 2527 (1994).
9. J. F. Kenney, V. A. Kutscherov, N. A. Bendelian, and V. A. Alexeev, Proc. Natl. Acad. Sci. USA **99**, 10 976 (2002).
10. P. Denies, Earth-Sci. Rev. **58**, 247 (2002).
11. O. Yu. Batalin, A. I. Brusilovskii, and M. Yu. Zakharov, *Phase Equilibria in Systems of Natural Hydrocarbons* (Nedra, Moscow, 1992) [in Russian].
12. E. G. Areshev, *Petroliferous Basins of the Pacific Mobile Belt* (AVANTI, Moscow, 2004) [in Russian].
13. A. E. Kontorovich and V. S. Vyshemirskii, Dokl. Akad. Nauk **356**, 794 (1997) [Dokl. Earth Sci. **357**, 1154 (1997)].
14. I. K. Karpov, V. S. Zubkov, V. A. Bychinskii, and M. V. Artimenko, Geol. Geofiz. **39**, 754 (1998).
15. A. A. Marakushev, Vestn. Ross. Akad. Nauk **70**, 223 (2000).